Phase diagram and collective modes in Rashba spin–orbit coupled BEC: Effect of in-plane magnetic field*

Dong Dong(董 冬), Zou Xu-Bo(邹旭波)†, and Guo Guang-Can(郭光灿)

Key Laboratory of Quantum Information, University of Science and Technology of China, Hefei 230026, China

(Received 8 March 2015; revised manuscript received 14 April 2015; published online 18 May 2015)

We studied the system of pure Rashba spin–orbit coupled Bose gas with an in-plane magnetic field. Based on the mean field theory, we obtained the zero temperature phase diagram of the system which exhibits three phases, plane wave (PW) phase, striped wave (SW) phase, and zero momentum (ZM) phase. It was shown that with a growing in-plane field, both SW and ZM phases will eventually turn into the PW phase. Furthermore, we adopted the Bogoliubov theory to study the excitation spectrum as well as the sound speed.

Keywords: Rashba spin–orbit coupling, excitation spectrum, in-plane magnetic field

PACS: 67.85.Fg, 05.30.Jp, 03.75.Mn **DOI:** 10.1088/1674-1056/24/7/076701

1. Introduction

The synthetic gauge field, which is induced by the atom–light interaction in cold atom gases, has been paid great attention since Spielman's group realized the spin–orbit coupling (SOC) experimentally in 2009.[1] Different from the situation in solid materials where SOC is studied only in the fermonic system, the synthetic gauge field in dilute cold atom gases can be applied to a bosonic system and is highly tunable, so a variety of works[2–9] have been carried out relating to this topic, including the Rashba type SOC,[10,11] the exotic superfluidity in SOC,[12] the SOC in an optical lattice,[13,14] etc.

The Rashba type SOC is an interesting configuration in the bosonic system, in which the spin is coupled to two directions in the momentum space and thus has a higher symmetry compared with the standard Raman-induced SOC realized in Ref. [1]. Although it has not been experimentally realized yet, there are several theoretical proposals for its realization.[15–17] In Refs. [10] and [11], it is shown that in the Rashba type SOC, the minima of the single particle energy form a continuous circle in the momentum space with infinite degeneracy, and two phases, the plane wave (PW) phase and the striped wave (SW) phase (also called the standing wave phase), can be identified due to the competition between the inter-component interaction and the intra-component interaction. Furthermore, a new fully polarized phase, the ZM phase in which the condensate has zero momentum, is found in the large repulsive inter-component interaction area with phase separation towards the SW phase.[18] Moreover, half vortex states and other phases have been predicted for the SOC condensate inside a harmonic trap.[11,19] However, in those works, the effect of an additional in-plane magnetic field has not been studied. In this paper, we will take the in-plane magnetic field into account and study its influence on the ground states and the phase diagram. We first demonstrate that with an in-plane magnetic field, the minima of the single particle energy turn into one single point on the continuous circle in the momentum space. Moreover, with an increasing additional magnetic field, the condensate in the ZM phase will gradually change the particular momentum that it occupies away from zero and eventually enters the PW phase. For the SW case, though the condensate will still have the structure of superposition of two plane wave states with opposite momenta, the ratio of the plane wave state which occupies the single particle minimum will increase with the increasing magnetic field while the one with the opposite momentum will decrease and eventually disappear, turning the system into the PW phase as well.

2. Phase diagram

We start with the single particle Hamiltonian describing the spin-1/2 bose gas with pure Rashba SOC in an additional magnetic field in the x direction (set $\hbar = m = 1$ for simplicity)

$$H_{\rm s} = \frac{1}{2}[(k_x - \lambda\sigma_x)^2 + (k_y - \lambda\sigma_y)^2] - h\sigma_x, \tag{1}$$

where σ_i are the Pauli matrices, λ is the Rashba coupling strength, and $h \geq 0$ characterizes the intensity of the additional magnetic field in the x direction. This single particle Hamiltonian is exactly solvable and the eigenvalues in terms of $\boldsymbol{p}$ are

$$\varepsilon_{\pm}(\boldsymbol{p}) = \frac{\boldsymbol{p}^2 + 2\lambda^2}{2} \pm \sqrt{(h + \lambda p_x)^2 + \lambda^2 k_y^2}, \tag{2}$$

which includes two helicity branches for spin parallel and antiparallel. Compared with the pure Rashba case, adding a magnetic field changes the minima of the spectrum from a ring in

*Project supported by the National Natural Science Foundation of China (Grant No. 10774088).

†Corresponding author. E-mail: xbz@ustc.edu.cn

© 2015 Chinese Physical Society and IOP Publishing Ltd

the momentum space $|\boldsymbol{k}| = \lambda$ to a single point of $k_x = \lambda, k_y = 0$ on the ring (see Fig. 1), which means that the condensation changes from a superposition of states with momenta on the degenerate ring to a particular single particle state.

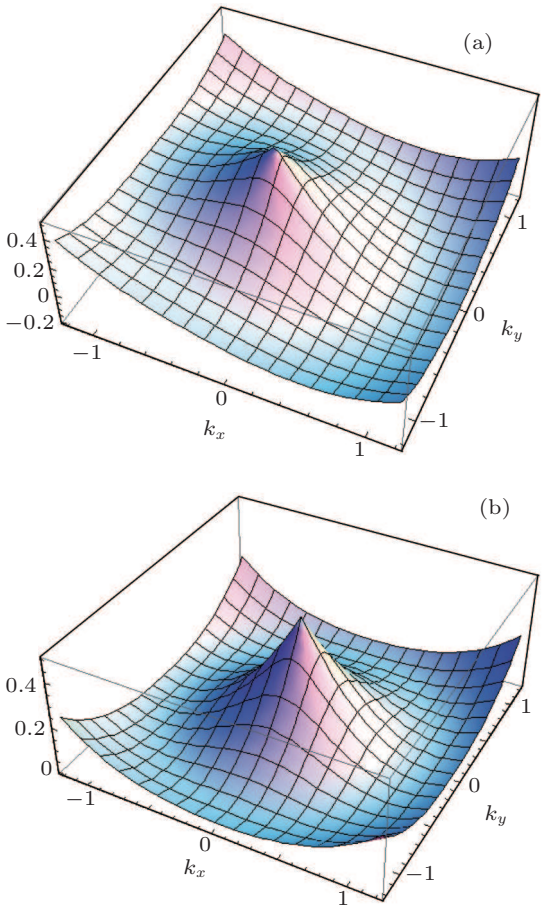


Fig. 1. (color online) The single particle ground state energy (the lower branch of the spectrum) of the system at (a) $h = 0.2\lambda^2$ and (b) $h = 0$.

For the many-body case of a dilute bose-1/2 gas with N particles enclosed in volume V, the interactions between atoms can be described by

$$H_{\rm int} = \frac{1}{2}\sum_{\sigma={\rm a,b}}\int {\rm d}^3 r g_{\sigma_1\sigma_2}\hat{\psi}^\dagger_{\sigma_1}\hat{\psi}^\dagger_{\sigma_2}\hat{\psi}_{\sigma_2}\hat{\psi}_{\sigma_1}, \tag{3}$$

where $\hat{\psi}_\sigma$ is the field operator, and $g_{\sigma_1\sigma_2}$ are the relative coupling constants in different spin channels. For simplicity, we consider the spin symmetric case $g_{\rm aa} = g_{\rm bb} = g$, the above equation can be rewritten as

$$H_{\rm int} = \int {\rm d}^3 r\left(\frac{G_1}{\bar{n}}\hat{n}^2 + \frac{G_2}{\bar{n}}\hat{S}_z^2\right), \tag{4}$$

where $G_1 = \bar{n}(g+g_{\rm ab})/4, G_2 = \bar{n}(g-g_{\rm ab})/4, \hat{n} = \hat{n}_{\rm a} + \hat{n}_{\rm b}, \hat{S}_z = \hat{n}_{\rm a} - \hat{n}_{\rm b}$ ($\hat{n}_\sigma = \hat{\psi}^\dagger_\sigma\hat{\psi}_\sigma, \sigma = {\rm a,b}$), and $\bar{n} = N/V$ is the average density.

Like the pure Rashba case, following the procedure in Ref. [18], the ground state and energy can be determined using a variational procedure by assuming the spinor wave function

$$\begin{pmatrix}\psi_{\rm a}\\ \psi_{\rm b}\end{pmatrix} = \sqrt{\bar{n}}\left[C_1\begin{pmatrix}\cos\theta\\ \sin\theta\,{\rm e}^{{\rm i}\phi}\end{pmatrix}{\rm e}^{{\rm i}\boldsymbol{k}\cdot\boldsymbol{r}} + C_2\begin{pmatrix}\sin\theta\\ -\cos\theta\,{\rm e}^{{\rm i}\phi}\end{pmatrix}{\rm e}^{-{\rm i}\boldsymbol{k}\cdot\boldsymbol{r}}\right], \tag{5}$$

where $\boldsymbol{k}$ represents the canonical momentum of the BEC. For a known value of average density $\bar{n}$, the variational parameters are θ, ϕ, C_1, C_2, and k with their values limited by the normalization constraints $|C_1|^2 + |C_2|^2 = 1$ and $\theta \in [0, \pi/2], \phi \in [0, \pi]$. Inserting Eq. (5) into Eqs. (1) and (4), we obtain

$$\begin{aligned}\varepsilon =\ & \lambda^2 + \frac{k^2}{2} - \lambda\sin 2\theta(k_x\cos\phi + k_y\sin\phi)\\ & - h\sin 2\theta(C_1^2 - C_2^2) + G_1\\ & + G_2(2C_1^2C_2^2\sin^2 2\theta + (C_1^2 - C_2^2)^2\cos^2 2\theta).\end{aligned} \tag{6}$$

By minimizing the energy respect to k, we simply have $k_x = \lambda\sin 2\theta\cos\phi$ and $k_y = \lambda\sin 2\theta\sin\phi$. By assuming $|C_1|^2 = (1-t)/2$ and $|C_2|^2 = (1+t)/2$, where $t \in [0,1]$, the energy per particle ε takes the form

$$\begin{aligned}\varepsilon =\ & \lambda^2 - \frac{\lambda^2}{2}\sin^2 2\theta + G_2 t^2(1 - \sin^2 2\theta) + th\sin 2\theta\cos\phi\\ & + G_1 + \frac{G_2(1-t^2)}{2}\sin^2 2\theta.\end{aligned} \tag{7}$$

The minimum of Eq. (7) is obtained at $\cos\phi = 1$ when $t < 0$ and $\cos\phi = -1$ when $t > 0$, we consider only the $\cos\phi = -1$ and $t > 0$ cases, since these two cases are equivalent.

Actually equation (7) is a quadratic function of t and $\sin 2\theta$, so the minimum and the ground state can be analytically calculated. Depending on the relevant parameters h, G_2, and λ, the minimum occurs at $k_x < \lambda$ with $t = 1$ and also $k_x = \lambda$ with $t = 1$ or $t < 1$. Therefore the system has three distinct phases and the phase diagram is shown in Fig. 2.

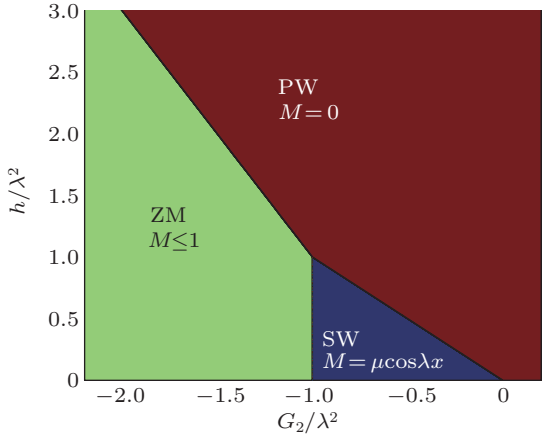


Fig. 2. (color online) The ground state phase diagram of the Rashba SOC Bose gas with additional magnetic field h in the x direction. These three phases have different spin polarization M.

(i) The ZM phase It is a polarized condensate which occupies the particular momentum $k_x = h\lambda/(-2G_2 - \lambda^2), k_y = k_z = 0$. For the $h = 0$ case, it is the ZM phase referred in Ref. [18] and the system enters this phase when $G_2 < -\lambda^2$

with phase separation from SW. When h becomes larger, $h > -2G_2 - \lambda^2$, the system enters the plane wave phase. The spin polarization of the phase is $M = \sqrt{1-k_x^2/\lambda^2}$ and the density is uniform. The energy of the ZM phase is

$$\varepsilon_{\rm ZM} = G_1 + G_2 + \lambda^2 + \frac{h^2}{4G_2 + 2\lambda^2}. \tag{8}$$

The corresponding wave function is

$$\psi_{\rm ZM} = \sqrt{\bar{n}} \begin{pmatrix} \cos\theta_h \\ \sin\theta_h \end{pmatrix} e^{ik_x x}, \tag{9}$$

where $\theta_h = \arcsin(k_x/\lambda)/2$ gradually changes from 0 to $\pi/2$, and k_x, the single momentum that it occupies, increases from 0 to λ as h increases. The ZM phase is a pure interaction consequence, which shows strong contrast with the single particle picture at the $h = 0$ case, even a small in-plane field h changes the situation and makes the atoms condensate at a non-zero momentum.

(ii) The SW phase The atoms condensate into a superposition of two plane wave states with opposite wave vectors $k_x = \pm\lambda$, the system enters this phase when $-\lambda^2 < G_2 < 0$ at $h = 0$ and forms a standing wave pattern. An increasing h would make the system transit into the plane wave phase, which occurs at $h > -G_2$. The condensate in this phase has the spin polarization in the form of stripes $M = \sqrt{1-(h/G_2)^2}\cos 2\lambda r$, which is the most striking feature of this phase. The ground state energy of this phase is

$$\varepsilon_{\rm SW} = G_1 + \frac{G_2}{2} + \frac{h^2}{2G_2} + \frac{\lambda^2}{2}, \tag{10}$$

and the wave function is

$$\psi_{\rm SW} = \sqrt{\bar{n}}\left[C_1 \begin{pmatrix} 1 \\ 1 \end{pmatrix} e^{i\lambda x} + C_2 \begin{pmatrix} 1 \\ -1 \end{pmatrix} e^{-i\lambda x}\right], \tag{11}$$

where $|C_1|^2 = (1 - h/G_2)/2$ and $|C_2|^2 = (1 + h/G_2)/2$. As h increases, the SW state slowly shifts its $-\lambda$ part to λ part and eventually becomes the PW state, while the competition with the ZM phase remains the same as the $h = 0$ case, and the transition occurs at $G_2 = -\lambda^2$ despite the phase separation.

(iii) The PW phase In the $h = 0$ case, the system enters this phase only when $G_2 > 0$. However, in a large additional field, the system originally in the above two phases also enters this plane wave phase. As discussed above, the critical value is $h = -G_2$ for the PW–SW transition and $h = -2G_2 - \lambda^2$ for the PW–ZM transition,. In this phase, the condensation is in the single plane wave state with momentum $k_x = \lambda, k_y = 0, k_z = 0$ and the spin polarization M is zero. The average energy reads

$$\varepsilon_{\rm PW} = G_1 - h + \frac{\lambda^2}{2}, \tag{12}$$

and the wave function is

$$\psi_{\rm PW} = \frac{\sqrt{2\bar{n}}}{2} \begin{pmatrix} 1 \\ 1 \end{pmatrix} e^{i\lambda x}. \tag{13}$$

It is noticed that the density of the ZM phase is not homogeneous, a phase separation (PS) may appear between the ZM phase and the other phases as in the $h = 0$ case.[18] The precise boundaries for the phase transitions can be determined by imposing the chemical potential $\mu = \partial n\varepsilon/\partial n$ and the pressure $P = \bar{n}(\mu - \varepsilon)$ being equal in the two phases. The chemical potentials in the three phases take the form

$$\begin{aligned} \mu_{\rm PW} &= 2G_1 - h + \frac{\lambda^2}{2}, \\ \mu_{\rm ZM} &= \lambda^2 + 2G_1 + 2G_2 + \frac{k_x^2}{2}, \quad k_x = \frac{h\lambda}{-2G_2 - \lambda^2}, \\ \mu_{\rm SW} &= 2G_1 + G_2 + \frac{\lambda^2}{2}. \end{aligned} \tag{14}$$

We find that the phase separation appears only on the ZM–SW transition like the $h = 0$ case, and with smaller $g_{\rm ab}/g$ or bigger h, the PS region becomes narrower, see Fig. 3.

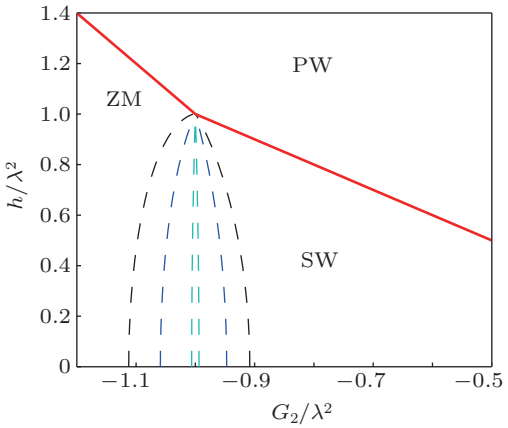


Fig. 3. (color online) Illustration of phase separation on the ZM–SW transition. The dashed lines show the PS area: black for $g_{\rm ab}/g = 3$, blue for $g_{\rm ab}/g = 2$, and light blue for $g_{\rm ab}/g = 1.1$.

3. Collective modes

In the following, we calculate the elementary excitations of the system using the Bogoliubov theory. First we add a perturbation

$$V_P = -P e^{\boldsymbol{q}\cdot\boldsymbol{r} - \omega t} + \text{H.c}$$

to the single particle Hamiltonian. Then the elementary excitations can be calculated by diagonalizing the following time-dependent Gross–Pitaevskii (G–P) equation:

$$i\partial_t \psi = \left[H_{\rm s} + V_P + \frac{2G_1}{n}(\psi^\dagger\psi) + \frac{2G_2}{n}(\psi^\dagger\sigma_z\psi)\right]\psi, \tag{15}$$

where $H_{\rm s}$ is the single-particle Hamiltonian in Eq. (1). We also know that for the PW and the ZM phases, the ground state density is uniform, so the spinor wave function can be written in the following form:

$$\begin{aligned} \psi = \sqrt{n}\Bigg[& \begin{pmatrix} \cos\theta \\ \sin\theta \end{pmatrix} e^{ik_x x} + \begin{pmatrix} u_\uparrow(\boldsymbol{r}) \\ u_\downarrow(\boldsymbol{r}) \end{pmatrix} e^{-i\omega t} \\ & + \begin{pmatrix} v_\uparrow^*(\boldsymbol{r}) \\ v_\downarrow^*(\boldsymbol{r}) \end{pmatrix} e^{i\omega t}\Bigg] e^{i\mu t}. \end{aligned} \tag{16}$$

Using Bogoliubov amplitudes u and v, we find the following matrix to be diagonalized in the PW phase:

$$B_{\rm PW}=\begin{pmatrix} H^+ & b^+ + {\rm i}\lambda q_y & -\frac{g}{2} & -\frac{g_{\rm ab}}{2} \\ b^+ - {\rm i}\lambda q_y & H^+ & -\frac{g_{\rm ab}}{2} & -\frac{g}{2} \\ -\frac{g}{2} & -\frac{g_{\rm ab}}{2} & H^- & b^- + {\rm i}\lambda q_y \\ -\frac{g_{\rm ab}}{2} & -\frac{g}{2} & b^- - {\rm i}\lambda q_y & H^- \end{pmatrix}, \tag{17}$$

where $H^\pm = -\lambda^2 - \frac{q^2}{2} - \frac{g}{2} \pm \omega \mp \lambda q_x - h$ and $b^\pm = \lambda^2 - \frac{g_{\rm ab}}{2} + h \pm \lambda q_x$. In the ZM phase, the matrix is

$$B_{\rm ZM}=\begin{pmatrix} H_1^+ & c^+ + {\rm i}\lambda q_y & m_1 & d \\ c^+ - {\rm i}\lambda q_y & H_2^+ & d & m_2 \\ m_1 & d & H_1^- & c^- + {\rm i}\lambda q_y \\ d & m_2 & c^- - {\rm i}\lambda q_y & H_2^- \end{pmatrix}, \tag{18}$$

where

$$\begin{aligned} H_1^\pm &= -q^2/2 + (g - g_{\rm ab})\sin^2\theta_h - g\cos^2\theta_h \pm \omega \mp \lambda q_x, \\ H_2^\pm &= -\frac{q^2}{2} + (g - g_{\rm ab})\cos^2\theta_h - g\sin^2\theta_h \pm \omega \mp \lambda q_x, \\ c^\pm &= -\frac{g}{2}\sin 2\theta_h \pm \lambda q_x, \quad d = -\frac{g_{\rm ab}}{2}\sin 2\theta_h, \\ m_1 &= -g\cos^2\theta_h, \quad m_2 = -g\sin^2\theta_h. \end{aligned}$$

We diagonalize the two matrices to obtain the elementary excitations as shown in Figs. 4 and 5. In the PW phase, we can easily find that the excitations have two branches as displayed in Fig. 4, which are gapless in the x direction and gapped in the y direction like the $h = 0, G_2 \geq 0$ case.[12,20] A more close look at the picture, we find that the lower branch is symmetric in the x direction, which is confirmed in the sound velocity calculated by $\lim_{p\to 0} E_p^- = cp$,

$$c_{\rm pw} = \sqrt{2G_1\left(1 - \frac{\lambda^2\cos^2\beta}{-h+\lambda^2}\right)}, \tag{19}$$

where $\beta = \arccos(p_y/p)$. It shows that h does not affect the sound velocity along the x direction.

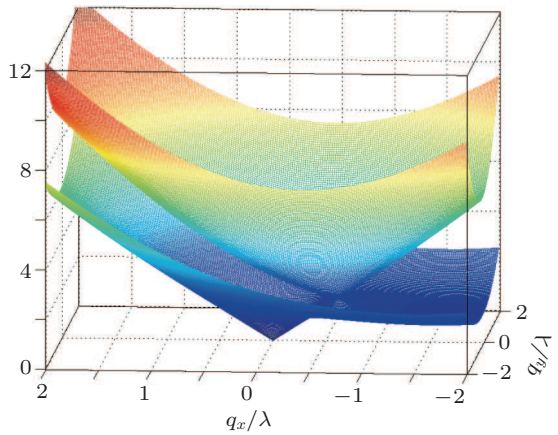


Fig. 4. (color online) Elementary excitations in the PW area, where $G_1 = 3.75\lambda^2$, $G_2 = -1.2\lambda^2$, and $h = 2\lambda^2$.

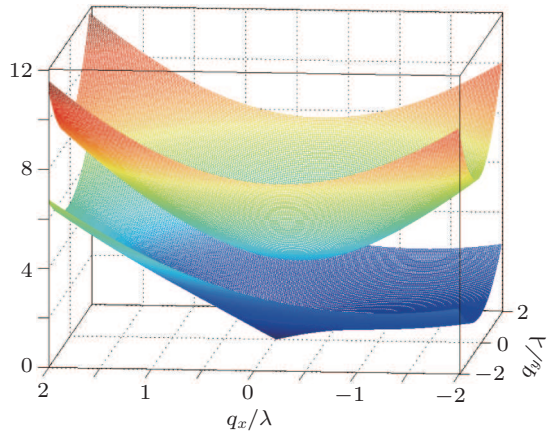


Fig. 5. (color online) Elementary excitations in the ZM area, where $G_1 = 3.75\lambda^2$, $G_2 = -1.2\lambda^2$, and $h = 1\lambda^2$.

In the ZM phase, the higher branch possesses a gap which is just the energy cost to overcome the effective Zeeman field.[18] The h also breaks the rotation symmetry and makes the lower branch higher when q is along the x direction and lower when q turns to the opposite direction, which is also clearly shown in the anisotropic sound velocity

$$c_{\rm zm} = k_x\cos\alpha + \sqrt{g\bar{n}\left(1 - \frac{2\lambda^2(\cos^2\alpha + \cos^2\beta)}{\bar{n}(g_{\rm ab} - g)}\right)}, \tag{20}$$

where $\alpha = \arccos(p_x/p)$ and $k_x = h\lambda/(-2G_2 - \lambda^2)$ increases with h. The sound velocity reaches its maximum when the phonon propagates in the x direction and minimum in the opposite direction.

4. Conclusion

We studied a system of pure Rashba spin–orbit coupled Bose gas with an in-plane magnetic field based on the mean field theory. We identified three distinct phases (PW phase, SW phase, and ZM phase) in zero temperature and found that with a growing in-plane magnetic field, both SW and ZM phases will eventually turn into the PW phase. Furthermore, we adopted the Bogoliubov theory to study the excitation spectrum as well as the sound speed.

References

[1] Lin Y J, Jimenez-Garcia K and Spielman I B 2011 *Nature* **471** 83
[2] Dalibard J, Gerbier F, Juzeliunas G and Ohberg P 2011 *Rev. Mod. Phys.* **83** 1523
[3] Goldman N, Juzeliunas G, Ohberg P and Spielman I B 2014 *Rep. Prog. Phys.* **77** 126401
[4] Zhou X F, Li Y, Cai Z and Wu C J 2013 *J. Phys. B: At. Mol. Opt. Phys.* **46** 134001
[5] Zhang S and Ho T L 2011 *Phys. Rev. Lett.* **107** 150403
[6] Li Y, Martone G I and Stringari S 2014 arXiv: 1410.5526
[7] Galitski V and Spielman I B 2013 *Nature* **494** 49
[8] Wang X, Tan R B, Du Z J, Zhao W Y, Zhang X F and Zhang S G 2014 *Chin. Phys. B* **23** 070308
[9] Xie W F, He Y Z and Bao C G 2015 *Chin. Phys. B* **24** 060305
[10] Wang C, Gao C, Jian C M and Zhai H 2010 *Phys. Rev. Lett.* **105** 160403
[11] Wu C J, Mondragon-Shem I and Zhou X F 2011 *Chin. Phys. Lett.* **28** 097102
[12] Zhu Q Z, Zhang C W and Wu B 2012 *Euro. Phys. Lett.* **100** 50003
[13] Radic J, Ciolo A D, Sun K and Galitski V 2012 *Phys. Rev. Lett.* **109** 085303
[14] Cai Z, Zhou X F and Wu C J 2012 *Phys. Rev. A* **85** 061605
[15] Dalibard J, Gerbier F, Juzeliunas G and Ohberg P 2011 *Rev. Mod. Phys.* **83** 1523
[16] Xu Z F and You L 2012 *Phys. Rev. A* **85** 043605
[17] Anderson B M, Spielman I B and Juzeliunas G 2013 *Phys. Rev. Lett.* **111** 125301
[18] Yu Z Q 2013 *Phys. Rev. A* **87** 051606
[19] Sinha S, Nath R and Santos L 2011 *Phys. Rev. Lett.* **107** 270401
[20] Xu X Q and Han J H 2012 *Phys. Rev. Lett.* **108** 185301